23. Cells in 100-mm tissue culture plates were incubated with ^{35}S-labeled methionine and cysteine (0.1 mCi/ml; specific activity, 1150 Ci/ml; Du Pont Biotechnology Systems) in heparin (50 μg/ml) for 4 hours as described (*2*). Conditioned medium was concentrated 20-fold in a Centricon-10 microconcentrator (Amicon) and immunoprecipitated with nonimmune or HGF-neutralizing antiserum. Immunoprecipitates were absorbed onto Gamma-bind G agarose (Genex) and washed three times with 10 mM tris-HCl buffer containing 150 mM NaCl, 0.05% Tween 20, 0.1% SDS, 1% NP-40, 1 mM EDTA, and 10 mM KCl. Samples were analyzed under reducing (with 100 mM β-mercaptoethanol) and nonreducing conditions with 10% or 14% SDS-PAGE. Gels were fixed, treated with enlightening solution (Du Pont Biotechnology Systems), dried, and exposed to Kodak AR film at −70°C.
24. C. R. Merril, D. Goldman, S. A. Sedman, M. H. Ebert, *Science* **211**, 1437 (1981).
25. J. S. Rubin *et al.*, *Proc. Natl. Acad. Sci. U.S.A.* **86**, 802 (1989).
26. Total and poly(A)$^+$ RNA were isolated as described (*17*). After separating samples by electrophoresis with 1% denaturing formaldehyde agarose gels, we transferred the samples to nitrocellulose filters (*17*). Blots were hybridized at 42°C for 12 hours to ^{32}P-labeled randomly primed DNA probes in 40% formamide, 6× saline sodium citrate (SSC), 5× Denhardt's solution, 50 mM sodium phosphate (pH 6.8), and sonicated salmon sperm DNA (250 μg/ml). After the hybridization reaction, we washed the filters twice in 1× SSC and 0.1% SDS at room temperature and in 0.1× SSC and 0.1% SDS at 55°C. Filters were dried and exposed to x-ray films for 5 to 8 days at −70°C. Hybridization probes were generated by PCR and purified on low melting temperature agarose gels. The nucleotide sequence of each probe was numbered according to the HGF sequence of Miyazawa *et al.* (7) as follows: H/L (heavy and light chains), −24 to +2187; H, +189 to +1143; and L, +1475 to +2122.
27. For routine PCR (*18*), 0.5 μg of human genomic DNA and 5 ng of plasmid DNA were subjected to 30 cycles of amplification with the following cycling conditions: 1 min at 94°C, 2 min at 60°C, and 3 min at 72°C. For PCR cloning of genomic DNA, PCR was carried out with Bam HI linker primers, and amplified DNA fragments were digested with Bam HI. The resultant Bam HI fragments were purified on a low melting temperature agarose gel and subcloned into the M13mp18 vector for sequencing analysis (*19*). Primers used were as follows: P1, AGTACTGTGCAATTAAAACATGCG; P2, GTAGAAAAATGATTGTATGGACTGCTA; P3, AGGCACTGACTCCGAAC A GGATTCTTTCACCC AGGCATCTCCTCC; and P4, ATGGATCCTTATGTCTCGCATGTTTTAATGCACA.
28. The HGK/NK2 coding sequence was generated by PCR with the Bam HI linker primers P3 and P4 (Fig. 2A) and subcloned into the Bam HI site of the vector pCDV-1 (*20*) in both orientations. We sequenced the HGF/NK2 insert in a selected construct to ensure that the PCR product was correct. Plasmid DNA (10 μg each) was transfected by the calcium phosphate precipitation method (*21*) into COS-1 cells (*22*). At 48 hours, proteins in conditioned medium were processed for labeling, immunoprecipitation, and SDS-PAGE under reducing and nonreducing conditions as described (*23*).
29. Conditioned medium (6 liters) from SK-LMS-1 cells grown in 175-cm^2 T flasks were passed through a 0.5-μm filter (Millipore) and concentrated to 300 ml with a Pellicon cassette system with a 10-kD molecular mass cutoff (Millipore). Concentrated medium was loaded at a flow rate of ~150 ml/hour onto heparin-Sepharose resin (4-ml bed volume, Pharmacia) that had been equilibrated in 20 mM tris-HCl (pH 7.5) and 0.3 M NaCl. The sample was eluted with a modified linear gradient of increasing NaCl concentration. We subjected aliquots from each fraction to immunoblot analysis with antiserum to HGF (final dilution 1:500) to identify the presence of HGF/NK2. Pooled fractions were further resolved on a TSK G2000 sizing column (Pharmacia) in 20 mM tris-HCl (pH 6.8) and 1.0 M NaCl. The purity and identity of the HGF/NK2 protein were determined by silver-stain analysis (*24*) and immunoblotting under reducing and nonreducing conditions. Fractions containing >95% of HGF/NK2 were selected for biological analysis. Protein concentration was estimated by absorbance (A) measurements; we assumed that $A^{1\%}_{214} = 140$.
30. Microtiter plates (96-well) were coated with human fibronectin at 1 μg/cm^2 before we seeded the plates with B5/589 cells as described (*25*). The incorporation of [^{3}H]thymidine was determined during a 6-hour period beginning 16 hours after the addition of samples. Trichloroacetic acid–insoluble DNA was collected and counted. HGF was purified as reported (*2*), and human recombinant EGF was purchased from Upstate Biotechnology.
31. TSK-purified HGF/NK2 was iodinated by the chloramine-T method as described (*4*). This HGF/NK2 represented >99% of the labeled material in the preparation, as determined by SDS-PAGE analysis. Affinity cross-linking experiments were performed on six-well plates seeded with B5/589 cells at a density of 5 × 10^5 cells per well. HGF/NK2 (5 × 10^5 cpm; specific activity, ~200 μCi/μg) was added to each well with or without nonradioactive competitors in Hepes binding buffer [100 mM Hepes, 150 mM NaCl, 5 mM KCl, 1.2 mM $MgSO_4$, 8.8 mM dextrose, heparin (2 μg/ml), and 0.1% bovine serum albumin; pH 7.4]. After we incubated the cells at room temperature for 45 min, we washed them twice in cold Hepes saline (pH 7.4). Disuccinimidyl suberate (Pierce) in dimethyl sulfoxide was added to a final concentration of 250 μM and incubated for 15 min. Samples were quenched with 100 μl of a solution containing 20 mM tris, 100 mM glycine, and 1 mM EDTA for 1 min and then rinsed in Hepes saline. Cells were extracted with Laemmli sample buffer and resolved by 6.5% SDS-PAGE under reducing conditions. Gel was dried and exposed to x-ray film at −70°C unless otherwise indicated.
32. We thank W. Taylor for advice concerning cell culture work, R. Halaban for assaying HGF/NK2 activity on human melanocyte cells, C. Florio and E. Fortney for technical assistance, J. Thompson for photography, and N. Lichtenberg for preparation of the manuscript.

5 July 1991; accepted 15 August 1991

Regulation of a Segmentation Stripe by Overlapping Activators and Repressors in the *Drosophila* Embryo

DUSAN STANOJEVIC, STEPHEN SMALL, MICHAEL LEVINE*

Gene expression stripes in *Drosophila melanogaster* embryos provide a model for how eukaryotic promoters are turned on and off in response to combinations of transcriptional regulators. Genetic studies suggested that *even-skipped* (*eve*) stripe 2 is controlled by three gap genes, *hunchback* (*hb*), *Kruppel* (*Kr*), and *giant* (*gt*), and by the maternal morphogen *bicoid* (*bcd*). A direct link is established between binding sites for these regulatory proteins in the stripe 2 promoter element and the expression of the stripe during early embryogenesis. The *bcd* and *hb* protein binding sites mediate activation, whereas neighboring *gt* and *Kr* protein sites repress expression and establish the stripe borders. The stripe 2 element has the properties of a genetic on-off switch.

THE PAIR-RULE GENE *EVE* ENCODES A homeobox protein important in the segmentation process. Mutations in *eve* produce severe segmentation defects, including the complete loss of segment borders in the middle body region (*1*). The *eve* protein is first detected 2 hours after fertilization, when it is uniformly distributed in all nuclei. This general expression gives way to a series of seven stripes along the length of the embryo before cellularization (*2*).

Individual stripes are regulated by separate cis elements contained within the *eve* promoter. For example, the first 1.7 kb of *eve* 5′ flanking sequence drives the expression of a *lacZ* reporter gene only within the limits of stripes 2 and 7; a 480-bp deletion between −1.6 and −1.1 kb abolishes expression of stripe 2 (*3, 4*). Stripe 3 depends on sequences located between −3.8 and −3 kb. We focus here on the regulation of stripe 2.

Genetic studies suggest that a total of four segmentation genes are responsible for stripe 2 expression (Fig. 1A). There are anterior and posterior expansions of the stripe borders in gt^- or Kr^- embryos, respectively, whereas the stripe is abolished or reduced in bcd^- or hb^- embryos (*5*). The four genetic regulators of stripe 2 expression may act directly on the *eve* promoter and modulate its transcription because proteins encoded by all four genes bind with high affinity to sequences in the *eve* promoter that are essential for stripe 2 expression (*5, 6*) (Fig. 1B).

To test whether the *bcd, hb, Kr*, and *gt* protein binding sites in the *eve* promoter directly mediate the interactions predicted by the genetic studies, we used site-directed mutagenesis (7) to disrupt some of these sites in a fusion gene that contains 5.2 kb of *eve* 5′ flanking sequence. This *eve-lacZ* fusion normally drives equally intense expression of stripes 2, 3, and 7 (*3, 4*). In this way, stripes 3 and 7 served as internal controls for perturbations of stripe 2 expression (*8*).

D. Stanojevic, Department of Biological Sciences, Fairchild Center, Columbia University, New York, NY 10027.
S. Small and M. Levine, Biology Department, Center for Molecular Genetics, Bonner Hall, University of California, La Jolla, CA 92093.

*To whom correspondence should be addressed.

Deoxyribonuclease (DNase) I protection assays indicated that the mutagenized sites failed to bind proteins within the detection limits of the method (*9*). Unfortunately, because the bcd1 and kr3 binding sites extensively overlap (Fig. 1B), it was not possible to disrupt one of the sites without affecting the other. The mutation in the bcd1 site also impairs the binding of *Kr* protein to the kr3 site (*10*). The bcd1-kr3 mutation alone did not cause a discernible change in stripe 2 expression. Also, the removal of the bcd2 site alone had no effect on stripe 2 expression. However, an *eve-lacZ* fusion gene containing mutations in both the bcd1-kr3 sequence and the bcd2 site resulted in reduced expression of stripe 2 relative to stripe 3 (Fig. 2, A and B) (*11*). Mutations in the hb3 binding site cause a similar but less severe reduction in stripe 2 expression (*9, 10*).

There are three *gt* protein binding sites present in the stripe 2 element (*5*) (Fig. 1B). These were disrupted by the creation of two small deletions; one deletion removes the gt2 and gt3 sites, whereas the other eliminates the gt1 site (*12*). This double mutation caused expansions of the anterior border of stripe 2 to a variable extent (Fig. 2C) (*11*). Despite this altered pattern, the level of stripe 2 expression is essentially normal. Transformants containing a single mutation lacking only the gt1 site or the gt2 and gt3 sites showed lesser expansions of the stripe (*9, 13*).

A series of mutations were made in each of the six high-affinity *Kr* protein binding sites present in the stripe 2 element. One of the *eve-lacZ* fusion genes that was examined contains point mutations in the kr1, kr2, kr4, and kr6 binding sites, none of which overlap any of the *bcd* protein sites (*14*) (Fig. 1B). This quadruple mutant causes a slight expansion of the stripe 2 posterior border that results in a narrower gap between stripes 2 and 3 (Fig. 3, A and B). Mutations in all six high-affinity *Kr* protein sites caused a greater posterior expansion of the border, so that stripes 2 and 3 were nearly contiguous (Fig. 3C).

Genetic studies had failed to distinguish between direct and indirect regulatory interactions (*2, 4*). For example, the expansion of the posterior *eve* stripe 2 border observed in Kr^- embryos could be due to direct repression by *Kr* protein or to an indirect effect of altering the expression pattern of *hb* (*15*). Stripe 2 expression is lost in bcd^- embryos (*5*), but because *bcd* protein functions as a direct transcriptional activator of *hb* (*16*), it was unclear from the genetic studies whether *bcd* protein is a direct or indirect regulator of stripe 2. We have presented evidence that at least some of the *bcd, hb, gt*, and *Kr* protein binding sites present in the *eve* promoter are likely to directly regulate stripe 2 expression in the early embryo. Mutations in *bcd* or *hb* protein binding sites cause reduced expression of stripe 2 but do not alter stripe 2's normal spatial limits. In contrast, mutations in either the *gt* or *Kr* protein sites change the positions of the stripe borders. Thus, the *eve* stripe 2 promoter element may act as a genetic on-off switch that integrates the activities of the *bcd* and *hb* activators with overlapping *gt* and *Kr* repressors.

There is a potential discrepancy between the genetic model of stripe 2 expression and the results obtained with mutagenized *eve* promoters lacking *Kr* protein binding sites. Disruptions in all six high-affinity *Kr* protein sites lead to a relatively mild posterior expansion in the stripe border (Fig. 3C). A more dramatic expansion of the stripe is observed in Kr^- embryos (*2, 4, 5, 17*). This could be explained by the fact that there are numerous low-affinity *Kr* protein binding sites present in the stripe 2 element (Fig. 1B). None of these sites were disrupted in the present study, and it is conceivable that

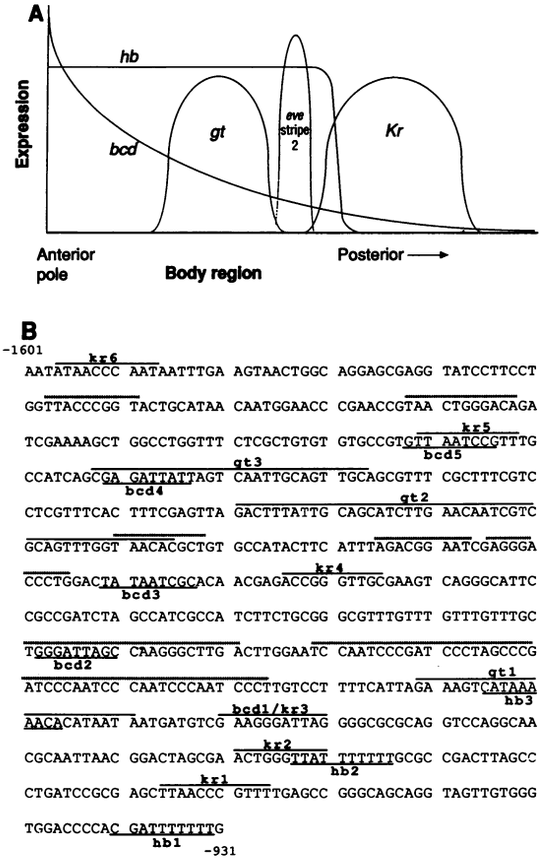

Fig. 1. Summary of stripe 2 regulation. (**A**) The limits of stripe 2 are shown relative to the expression domains of *bcd, hb, Kr*, and *gt*, which encode proteins distributed in broad, overlapping gradients (*5, 6, 20*). Both *bcd* and *hb* proteins function as transcriptional activators and define a broad domain in the anterior half of the embryo where the stripe 2 element can be activated. The borders of the stripe depend on selective repression by *gt* protein in anterior regions and *Kr* protein in posterior regions. (**B**) The nucleotide sequence of the stripe 2 promoter element. The sequence extends from −931 to −1601 bp upstream of the transcription start site. A 480-bp deletion from −1050 to −1530 bp completely abolishes the expression of the stripe (*4*). The locations of the *bcd, hb, gt*, and high-affinity *Kr* protein binding sites are indicated. The limits of these sites are based on DNase I protection assays and may extend beyond the core recognition sequences (*5, 6*). There is tight linkage of the *bcd* and *hb* activator sites (underlined sequences) and the *gt* and *Kr* repressor sites (indicated above the sequence). The broken lines indicate the locations of low-affinity *Kr* protein binding sites.

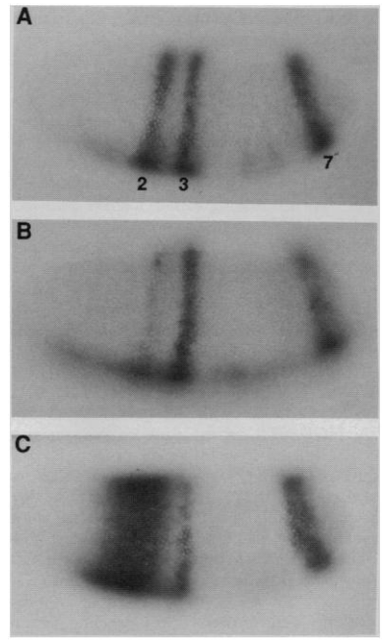

Fig. 2. Mutations in *bcd* and *gt* protein binding sites disrupt stripe 2 expression in embryos at nuclear division cycle 14. Embryos are oriented with anterior to the left and dorsal up. We hybridized all embryos with a *lacZ* antisense RNA probe to detect the expression of the reporter gene. (**A**) P-transformed embryo expressing the wild-type 5.2-kb *eve-lacZ* fusion gene. There is equally intense expression of stripes 2, 3, and 7. (**B**) Pattern obtained with the double mutant in the bcd1-kr3 sequence and the bcd2 site (*10*). There is a significant reduction in stripe 2 expression. (**C**) The expression pattern from an *eve-lacZ* fusion gene containing two small deletions that remove all three *gt* protein binding sites (*12*). There is an expansion of the anterior stripe 2 border (*13*).

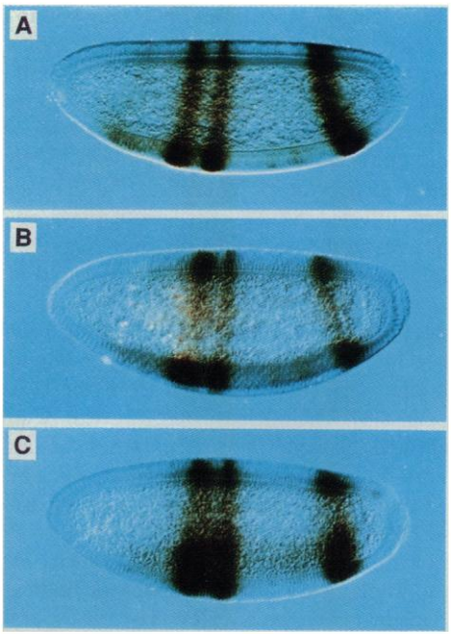

Fig. 3. *Kr* protein binding sites regulate the posterior stripe border. Embryos have completed cellularization and are oriented with anterior to the left and dorsal up. We stained the embryos with an antibody to β-galactosidase to detect the expression of the reporter gene. Stripes are numbered as in Fig. 2. (**A**) A P-transformed embryo expressing the wild-type 5.2-kb *eve-lacZ* fusion gene. Stripes 2, 3, and 7 are stained to the same extent. (**B**) Expression pattern from an *eve-lacZ* fusion containing point mutations in the kr1, kr2, kr4, and kr6 sites (*14*). There is a slight posterior expansion of stripe 2 that reduces the gap between stripes 2 and 3. (**C**) Expression of the *eve-lacZ* fusion gene containing point mutations in all six high-affinity *Kr* protein binding sites. There is a more pronounced expansion of stripe 2.

they can mediate repression by high concentrations of *Kr* protein.

The *gt* and *Kr* protein binding sites identified by in vitro assays correspond to authentic repressor sites in vivo. Because these sites overlap or are closely linked to the *bcd* and *hb* activator sites, it is likely that the *gt* and *Kr* proteins define the stripe borders through a short-range mechanism of repression. This could involve competitive binding to DNA, whereby the binding of *gt* or *Kr* protein precludes the binding of *bcd* and *hb* activators to overlapping sites. Alternatively, activators and repressors may bind to adjacent sites, but protein-protein interactions between the repressors and activators may "mask" the ability of activators to contact the transcription complex (*18*). Short-range repression could account for the autonomous action of individual stripe initiation elements. For example, the binding of *Kr* protein to stripe 2 sequences does not interfere with the activation of the stripe 3 element, which is activated in a region of the embryo containing high levels of the *Kr* repressor. Stripe 3 sequences do not contain any *Kr* protein binding sites (*6*) and map about 1.5 to 2 kb upstream of the stripe 2 element.

The interplay between activators and repressors observed here for the stripe 2 element may be a general component of eukaryotic enhancers. Although the early *Drosophila* embryo is a syncytium that permits the intermixing of regulatory factors by diffusion, there are numerous instances where small changes in the concentrations and combinations of factors might effect choices in cell fate. For example, in many cell lineages a common precursor gives rise to daughter cells that follow totally distinct differentiation pathways. Perhaps this involves a slight asymmetry in the concentrations or activities of regulatory factors inherited by daughter cells, which could be accomplished by the asymmetric partitioning of factors or distinct cell-cell interactions that cause slight differences in their activities. Once daughter cells have distinct combinations or concentrations of a common set of factors sharp on-off patterns in gene expression might be effected through enhancers analogous to the stripe 2 element.

REFERENCES AND NOTES

1. C. Nusslein-Volhard, H. Kluding, G. Jurgens, *Cold Spring Harbor Symp. Quant. Biol.* **50**, 145 (1985).
2. M. Frasch and M. Levine, *Genes Dev.* **1**, 981 (1987).
3. K. Harding, T. Hoey, R. Warrior, M. Levine, *EMBO J.* **8**, 1205 (1989).
4. T. Goto, P. Macdonald, T. Maniatis, *Cell* **57**, 413 (1989).
5. S. Small, R. Kraut, T. Hoey, R. Warrior, M. Levine, *Genes Dev.* **5**, 827 (1991).
6. D. Stanojevic, T. Hoey, M. Levine, *Nature* **341**, 331 (1989).
7. A 795-bp Xho I–Bal I *eve* promoter fragment extending from −1.7 to −0.9 kb upstream of the start site was subcloned into the pBluescript vector (Stratagene) and used for mutagenesis. Site-directed mutations were made with mutagenic oligonucleotides and the Bio-Rad mutagenesis kit. Single-stranded DNA templates were derived from the pBluescript vector. Oligonucleotides contained 25 to 40 bases with at least ten nucleotides of homology on either side of the mutagenized region. We made multiple mutants by simultaneously annealing two or more mutagenic oligonucleotides to the same DNA template. We exchanged all mutagenized fragments for wild-type sequences in the 5.2-kb *eve-lacZ* fusion gene (*3, 4*) by replacing wild-type fragments with the corresponding mutant templates in the pSSH7 vector (*19*), which contains a unique Not I restriction site. The *eve* promoter sequences were inserted into the pDM30 P-element vector at the unique Not I site (*19*). All *eve-lacZ* fusions were inserted into the pDM30 vector in the same orientation of transcription as the *rosy* marker gene. All mutations created within stripe 2 sequences were confirmed by restriction digestions, DNA sequencing, and DNase I footprint assays.
8. The *eve-lacZ* fusion genes were cloned into the pDM30 P-transformation vector and injected into $rosy^{506}$ embryos along with the Δ2,3 helper plasmid (*19*). For each construct, the following numbers of independent P-transformed lines were examined: Δhb3, two lines; Δbcd1-kr3, one line; Δbcd1 and bcd2, four lines; Δgt1, two lines; Δgt2 and gt3, five lines; Δgt1, gt2, and gt3, six lines; Δkr1, kr2, kr4, and kr6, five lines; and Δkr1, kr2, kr3, kr4, kr5, and kr6, seven lines. For most experiments, expression of the *lacZ* reporter gene was detected in P-transformed embryos by immunohistochemical staining with an antibody against β-galactosidase and visualized with a horseradish peroxidase–conjugated secondary antibody with the Elite kit (Vector Laboratories).
9. D. Stanojevic, unpublished results.
10. We used the following mutagenic oligonucleotides to create mutations in *bcd* and *hb* protein binding sites (the altered bases are in italics): bcd1-kr3, GATGTCGAAG*CATGCA*GGGGCGCGCAGG; bcd2, GTTTGTTTGCT*AGATCT*AGCCAAGGG-CTTG; and hb3, CATTAGGAAGT*CGCTAGCA*-CACATAATAAT. The mutation in the hb3 site does not affect the binding of *gt* protein to the overlapping gt1 site.
11. We visualized expression of the *lacZ* reporter gene by localizing RNA in whole-mount preparations of P-transformed embryos as described [D. Tautz and Pfeifle, *Chromosoma* **98**, 81 (1989); D. Kosman, Y. T. Ip, M. Levine, K. Arora, *Science* **254**, 118 (1991).
12. A 19-bp sequence that includes most of the gt1 recognition sequence was deleted and replaced by a 6-bp Sph I restriction site. A 100-bp sequence was deleted from the gt2 to gt3 region and also replaced with an Sph I site. This deletion nearly coincides with the sequences that are protected in DNase I footprint assays with high concentrations of *gt* protein. The neighboring bcd4 binding site (Fig. 1B) was left intact. The following mutagenic oligonucleotides were used (Sph I sites are in italic): gt1, GTCCTTTTCATTAGGG*CATGC*TAAT-GATGTCGAAGGG; and gt2 and gt3, GCCAT-CAGCGAGATTA*GCATGC*CTGTGCCAT-ACTTTC.
13. The intensity of stripe 2 is normal even though the gt1 deletion also removes the hb3 site. Disrupting the hb3 site in an otherwise normal *eve-lacZ* fusion results in reduced expression of the stripe. Thus, it would appear that the simultaneous loss of the gt1 site somehow compensates for the removal of hb3.
14. We used six oligonucleotides to mutagenize the *Kr* protein binding sites. Each of the oligonucleotides (except kr5) precisely removes the kr-binding consensus sequences and replaces it with a restriction site (in italics). The following oligonucleotides were used: kr1, CCTGATCCGCGA*GCTAGC*T-TGAGCCGGGCAGC; kr2, CGGACTAGCGAA-*CAGATCT*TTATTTTTTTGCGCCG; kr3, the oligonucleotide used for bcd1-kr3 in (*10*); kr4, CGCACAACGAGAC*GCATGC*GCGAAGT-CAGGGC; and kr6, GGGCGCAATATG*CAT-GC*TAATTTGAAGTAACTGGC. Because of the partial overlap between the kr5 and bcd5 binding sites (Fig. 1B), we designed the kr5 mutagenic oligonucleotide to abolish the binding of *Kr* protein without influencing the *bcd* protein binding. The oligonucleotide introduces the following four-base substitution (in italic): CGTGTTAATCC*AACG*-GCCATCAGCGAGATTATTAGTC.
15. H. Jackle, D. Tautz, R. Schuh, E. Seifert, R. Lehmann, *Nature* **324**, 668 (1986).
16. W. Driever and C. Nusslein-Volhard, *ibid.* **337**, 138 (1989); W. Driever, G. Thoma, C. Nusslein-Volhard, *ibid.* **340**, 363 (1989); G. Struhl, K. Struhl, P. Macdonald, *Cell* **57**, 1259 (1989).
17. R. Warrior and M. Levine, *Development* (*Cambridge*) **110**, 759 (1990).
18. M. Levine and J. L. Manley, *Cell* **59**, 405 (1989).
19. D. Mismer and G. Rubin, *Genetics* **116**, 565 (1987).
20. U. Gaul and H. Jackle, *Development* (*Cambridge*) **107**, 651 (1989).

21. We thank J. Jiang for help with the P transformations, G. Struhl for advice on antibody staining, and T. Hoey for the *eve* promoter sequence. D.S. thanks P. Stamenkovic and B. Stamenkovic for discussions and support. M.L. thanks P. Lawrence and E. Davidson for their encouragement. Supported by grant GM 34431 from the NIH.

29 July 1991; accepted 30 September 1991